OPTIMAL LIFTING RE-ENTRY BY REDUCED-ORDER APPROXIMATION

W. O'Dwyer, et al

Grumman Aerospace Corporation
Bethpage, New York

May 1973

RE-457

OPTIMAL LIFTING RE-ENTRY BY REDUCED-ORDER APPROXIMATION

May 1973

RESEARCH DEPARTMENT

GRUMMAN AEROSPACE CORPORATION
BETHPAGE NEW YORK

Unclassified

Security Classification

DOCUMENT CONTROL DATA - R & D

(Security classification of title, body of abstract and indexing annotation must be entered when the overall report is classified)

1. ORIGINATING ACTIVITY (Corporate author)	2a. REPORT SECURITY CLASSIFICATION
Grumman Aerospace Corporation	Unclassified
	2b. GROUP N/A

3. REPORT TITLE

Optimal Lifting Re-Entry by Reduced-Order Approximation

4. DESCRIPTIVE NOTES (Type of report and inclusive dates)

Research Report

5. AUTHOR(S) (First name, middle initial, last name)

W. O'Dwyer and H. Hinz

6. REPORT DATE	7a. TOTAL NO. OF PAGES	7b. NO. OF REFS
May 1973	~~57~~ 59	32

8a. CONTRACT OR GRANT NO.	9a. ORIGINATOR'S REPORT NUMBER(S)
b. PROJECT NO. N/A	RE-457
c.	9b. OTHER REPORT NO(S) (Any other numbers that may be assigned this report) None
d.	

10. DISTRIBUTION STATEMENT

Approved for Public release; distribution unlimited.

11. SUPPLEMENTARY NOTES	12. SPONSORING MILITARY ACTIVITY
None	None

13. ABSTRACT

A faster method for computing optimal three dimensional trajectories that maximize the landing footprint of a lifting re-entry vehicle has been developed. The method utilizes energy approximations based on the assumption that the flight path angle is small and the flight path angular rate is zero. Thus, the vertical component of lift is considered equal to the weight minus centrifugal relief, and the equation of motion are reduced in order from six to four. Because of this simplification, the classical indirect method of the calculus of variations is used to compute families of optimal solutions. Utilizing data corresponding to one of the space shuttle configurations, computations have been carried out for both unconstrained trajectories and for solutions that have aerodynamic heating rates and lift coefficients limited to specified values. During the investigation, several interesting analytical finds were uncovered that could be used as a basis for an onboard guidance scheme.

DD FORM 1 NOV 65 1473

Unclassified

Security Classification

14. KEY WORDS	LINK A		LINK B		LINK C	
	ROLE	WT	ROLE	WT	ROLE	WT

Grumman Research Department Report RE-457

OPTIMAL LIFTING RE-ENTRY BY REDUCED-ORDER APPROXIMATION

by

W. O'Dwyer

and

H. Hinz

System Sciences

May 1973

Approved by: Charles E. Mack, Jr.
Charles E. Mack, Jr.
Director of Research

ACKNOWLEDGMENT

The authors are indebted to Dr. Henry J. Kelley for the many helpful discussions and essential contributions to the development of this work. The original suggestion and early problem formulation were due to Dr. Kelley.

ABSTRACT

A faster method for computing optimal three dimensional trajectories that maximize the landing footprint of a lifting re-entry vehicle has been developed. The method utilizes energy approximations based on the assumption that the flight path angle is small and the flight path angular rate is zero. Thus, the vertical component of lift is considered equal to the weight minus centrifugal relief, and the equations of motion are reduced in order from six to four. Because of this simplification, the classical indirect method of the calculus of variations is used to compute families of optimal solutions. Utilizing data corresponding to one of the space shuttle configurations, computations have been carried out for both unconstrained trajectories and for solutions that have aerodynamic heating rates and lift coefficients limited to specified values. During the investigation, several interesting analytical finds were uncovered that could be used as a basis for an onboard guidance scheme.

TABLE OF CONTENTS

LIST OF ILLUSTRATIONS

INTRODUCTION

The introduction of energy approximation methods (Refs. 1-5) in 1944 has taken the science of high-speed aircraft performance calculations out of the realm of quasi-steady state analysis and into the framework of dynamics and the calculus of variations. These early attempts of extreme reduced-order approximations were applied only to two dimensional minimum time to climb problems and resulted in solutions that were plagued with subarcs consisting of unrealistic climbs and dives and large instantaneous flight path changes. Nevertheless, these solutions did resemble actual optimum flight paths and provided pilots with procedures for improved aircraft performance.

During the past twelve years the use of optimization techniques developed specifically for modern digital computers (Refs. 6-10) has gone to the other extreme, that of generating numerical solutions to complex three dimensional trajectory problems involving specified terminal conditions and inequality constraints on control and state variables. Although these solutions are realistic and provide a good reference of maximum possible performance, it is difficult to obtain an insight to the general characteristics of optimum aircraft maneuvers, and the high cost of computer usage makes it prohibitive to carry out any extensive aircraft parametric design studies. It would be desirable to have available a simpler and more efficient method that could overcome the preceding difficulties.

One promising approach that has been revived and extended is the energy-state or energy-maneuverability approximation (Refs. 11-14). The essential feature of the energy approximation is the reduction in order of the differential equations of motion, and

therefore a corresponding reduction in the Euler equations and the number of multiplier initial values. Although the reduction may not be sufficient for deriving analytic solutions it should facilitate use of the classical indirect method of the calculus of variations for efficiently computing many families of optimal solutions. This approach has been successfully carried out recently in a series of studies for calculating optimum turning maneuvers of aircraft at constant altitude (Refs. 15-18) and in three dimensions (Refs. 19-22).

The research investigation described in this report extends the energy type of approximation to the computation of optimum three dimensional trajectories that maximize the landing footprint of a lifting re-entry vehicle. The footprint may be considered as a locus of points; for each point the terminal condition is specified and the crossrange for any value of downrange has been maximized. The approximation is based on the assumption that the flight path angle γ is small ($\cos \gamma = 1$) and the angular rate $\dot{\gamma}$ is zero. Thus, the vertical component of lift is equal to the weight minus centrifugal relief. This has the effect of eliminating the skipping type of trajectory, and instead results in an equilibrium type of optimum glide. It should be noted that it is the long duration skipping motion that plays havoc with the convergence of iterative optimization techniques.

In addition to maximizing the landing footprint, the computer program also satisfies inequality constraints on underbody temperatures and maximum lift coefficient. No attempt has been made to optimize trajectories that terminate inside the footprint; however, this could conceivably be achieved by decreasing the value of the maximum allowable underbody temperature.

Because of the reduced order of the system, there is a problem of transitions from and to specified end conditions. As in the earlier minimum time to climb problems (Ref. 4), where energy is a state variable and altitude (or velocity) is employed as a control variable, a discontinuity in the control variable is mathematically permissible and results in instantaneous altitude/velocity changes. What is needed to correct these unrealistic maneuvers during re-entry is a method for getting on and off the optimal equilibrium glide path in an optimal manner. Since the reduced-order modeling eliminates the higher frequency motion, these fast transients have to be re-introduced and superimposed on the slowly varying motion in order to satisfy the boundary conditions. These transitions are suitable for treatment by singular perturbation theory and the "boundary layer" correction given as solutions of differential equations also of reduced order (Refs. 13 and 22-24). Some preliminary work along these lines has been carried out, but is not included in this report.

MATHEMATICAL MODEL

A computer program has been developed to optimize the three dimensional turning flight of a lifting re-entry vehicle, taking into account constraints placed on underbody temperatures and maximum lift coefficient. A spherical nonrotating earth with an inverse-square gravitational field and an exponential atmosphere is assumed. Rigid body dynamics are neglected, and throughout the flight the vehicle executes a coordinated turn maneuver of zero side force. Angle of attack and bank angle are the two control variables for the original model; however, for the reduced-order model, altitude replaces angle of attack as a control variable. The aerodynamic data are independent of Mach number.

Equations of Motion

The flight path equations before reduced-order approximations are made have the form

$$\dot{V} = -\frac{D}{m} - g \sin \gamma \tag{1}$$

$$\dot{\gamma} = \frac{L}{mV} \cos \mu - \frac{g}{V} \cos \gamma + \frac{V}{r} \cos \gamma \tag{2}$$

$$\dot{\chi} = \frac{L \sin \mu}{mV \cos \gamma} - \frac{V}{r} \cos \gamma \sin \chi \tan \varphi \tag{3}$$

$$\dot{r} = V \sin \gamma \tag{4}$$

$$\dot{\varphi} = -\frac{V}{r} \cos \gamma \cos \chi \tag{5}$$

$$\dot{\Lambda} = \frac{V}{r} \frac{\cos \gamma \sin \chi}{\cos \varphi} \tag{6}$$

where V is velocity, γ flight path angle, χ heading angle, r geocentric radius, φ latitude, Λ longitude (see Figs. 1 and 2), and the gravity $g = g_o r_o^2/r^2$. These equations are derived in Appendix A.

The specific energy E replaces velocity through the defining relationship:

$$E = \frac{V^2}{2g_o} - \frac{r_o^2}{r} \tag{7}$$

The choice of specific energy (foot-pounds per pound) as a state variable stems from the intuitive reasoning that E should be more slowly varying than either V or h. This would be particularly true if reduced-order approximations were not used, resulting in a skipping motion that can be thought of as an interchange of kinetic and potential energy about some equilibrium energy level. There is another reason for the preference of E over V. Because E decreases monotonically it is possible to reduce the order of the system by one by eliminating time and employing E as the independent variable. As shown in Appendix B, the order of the system is further reduced from four to three, thereby resulting in an analytical solution for the unconstrained case.

Substitution of Eq. (4) into (1) eliminates the $\sin\gamma$ terms from the equations of motion, and

$$\dot{V} = -\frac{D}{m} - \frac{g}{V}\dot{r} \tag{8}$$

This is significant, since the small angle approximation to be made for γ applies only to the $\cos\gamma$ terms, i.e., $\cos\gamma \approx 1$. The $\sin\gamma$ terms do not have to be approximated by $\sin\gamma \approx 0$ in order to derive exact expressions for E and $\dot{E}$. Differentiating Eq. (7) and combining with Eq. (8) results in

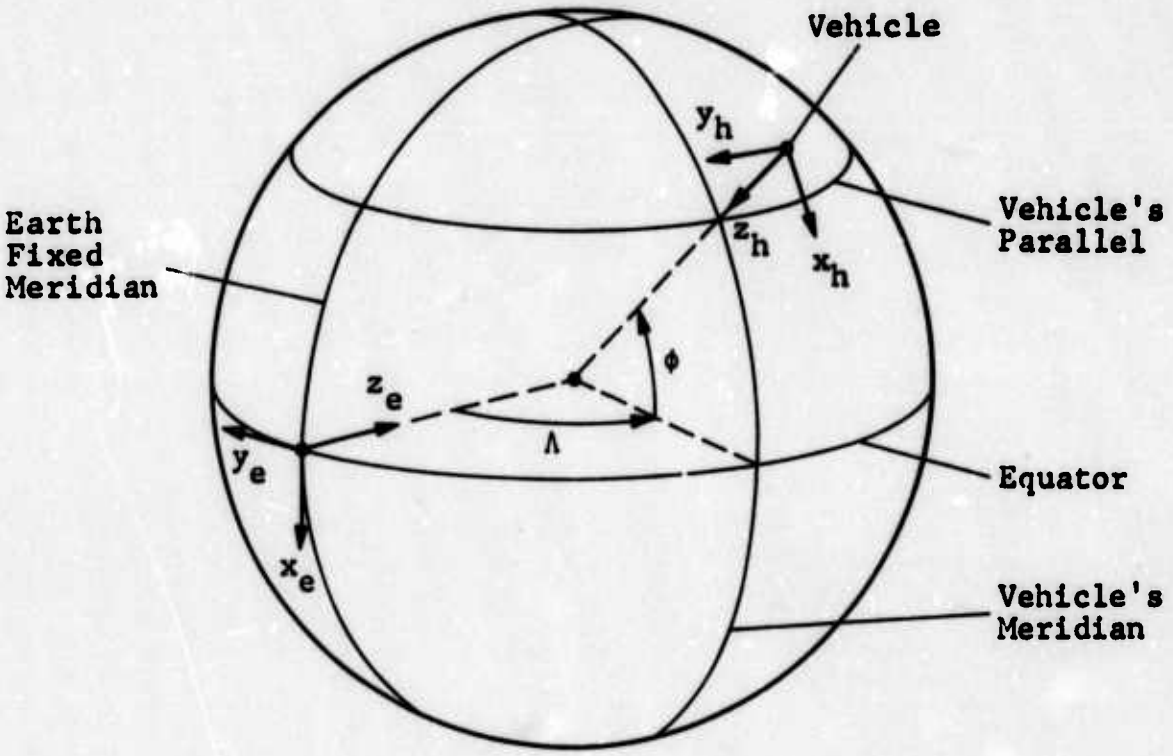

Fig. 1 Coordinate Systems for Flight Over Spherical Earth

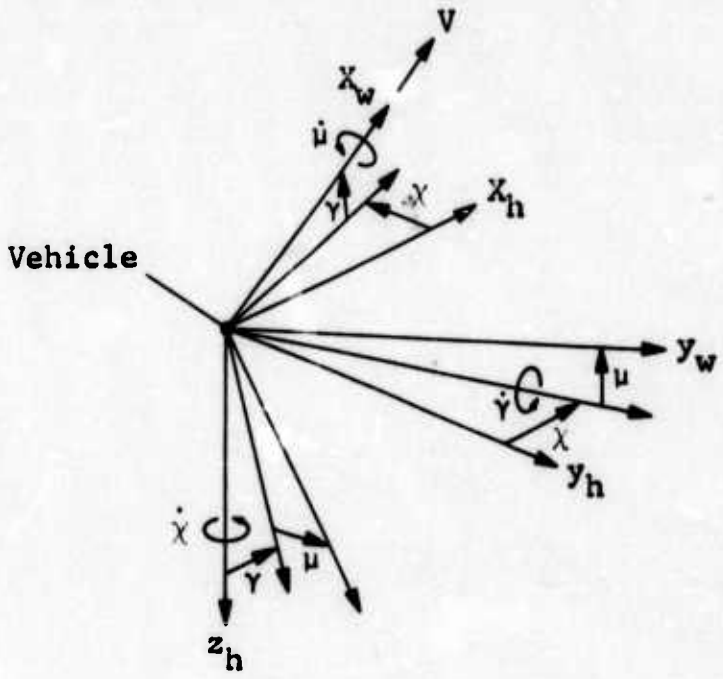

Fig. 2 System of Rotations from Local Horizon to Wind Axes

$$\dot{E} = -\frac{DV}{W}$$

where the weight $W = mg_o$, and V has been reduced to an ordinary variable defined by

$$V^2 = 2g_oE + \frac{2g_or_o^2}{r} \tag{9}$$

Based on the assumption that $\cos\gamma = 1$ and the angular rate $\dot{\gamma} = 0$, Eq. (2) is converted to an algebraic expression

$$L = \frac{WV}{g_o \cos\mu}\left[\frac{g_or_o^2}{Vr^2} - \frac{V}{r}\right] \tag{10}$$

where the altitude, $h = r - r_o$, is now employed as a control variable in addition to the angle of attack α and bank angle μ. The system of equations is reduced to fourth order:

$$\dot{E} = -\frac{DV}{W} \tag{11}$$

$$\dot{\chi} = \frac{g_oL\sin\mu}{WV} - \frac{V}{r}\sin\chi\tan\varphi \tag{12}$$

$$\dot{\varphi} = -\frac{V}{r}\cos\gamma \tag{13}$$

$$\dot{\Lambda} = \frac{V\sin\chi}{r\cos\varphi} \tag{14}$$

Because of Eq. (10) the three control variables are not independent of each other. Instead, h and μ are to be considered as the two primary control variables for the reduced-order system and α is to be determined from Eq. (10) and

$$\rho = \rho_o e^{-\beta h} \tag{15}$$

$$C_L = \frac{L}{\frac{1}{2}\rho V^2 S} \tag{16}$$

$$\alpha = .145 + .737 \tan(1.33\, C_L) \tag{17}$$

where the numerical expression for α versus C_L, with C_L limited to 0.535, corresponds to one of the early space shuttle orbiter configurations. Other equations and data are:

$$C_D = C_{D_o} + C_{D_{C_L^2}} C_L^2 \tag{18}$$

$$D = C_D \tfrac{1}{2}\rho V^2 S \tag{19}$$

where $C_{D_o} = .028$, $C_{D_{C_L^2}} = 1.69$, $W = 211{,}170$ lbs, $\rho_o = .0034$ slug/ft^3, $\beta = .0000421$ per ft, $r_o = 20{,}908{,}800$ ft, $g_o = 32.174$ ft/sec^2 and $S = 6100$ ft^2.

Boundary Conditions

At the start of re-entry $E_o = -11{,}717{,}000$ ft, $\gamma_o = \pi/2$ radians (heading east), $\varphi_o = 0$ (on the equator) and $\Lambda_o = 0$. The initial condition for E corresponds to a velocity of 24,000 ft/sec at an altitude of 40 nautical miles. However, since altitude is a control variable, to be determined optimally, only E_o remains fixed for each member of the footprint family, whereas the numerical values of altitude and velocity at $t = 0$ will vary while satisfying Eq. (7).

The final conditions of the turning flight re-entry are E_f = - 20,800,000 ft, γ_f is open and ψ_f and Λ_f are arrived at optimally such that the area of the landing footprint has been maximized. The value of E_f corresponds to a velocity of 2000 ft/sec at an altitude of 50,000 ft.

Inequality Constraints

The underbody temperature constraint is taken from Ref. 25, and for this investigation is considered to be typical for those cases where the boundary layer is assumed to be in thermal and chemical equilibrium. The constraint is given as boundaries in altitude-velocity space (Fig. 3) such that all underbody temperatures aft of the 20-foot station are limited to 1800°F. At higher altitudes the maximum temperature would be less than 1800°F and at lower altitudes the maximum temperature exceeds 1800°F. The boundaries are defined by laminar heating at the forward stations during the initial portion of entry. The break in the initial slope of the boundary is due to the onset and realization of turbulent heating at the aft stations.

An inequality constraint is also imposed on the lift coefficient which is limited to C_L = 0.535.

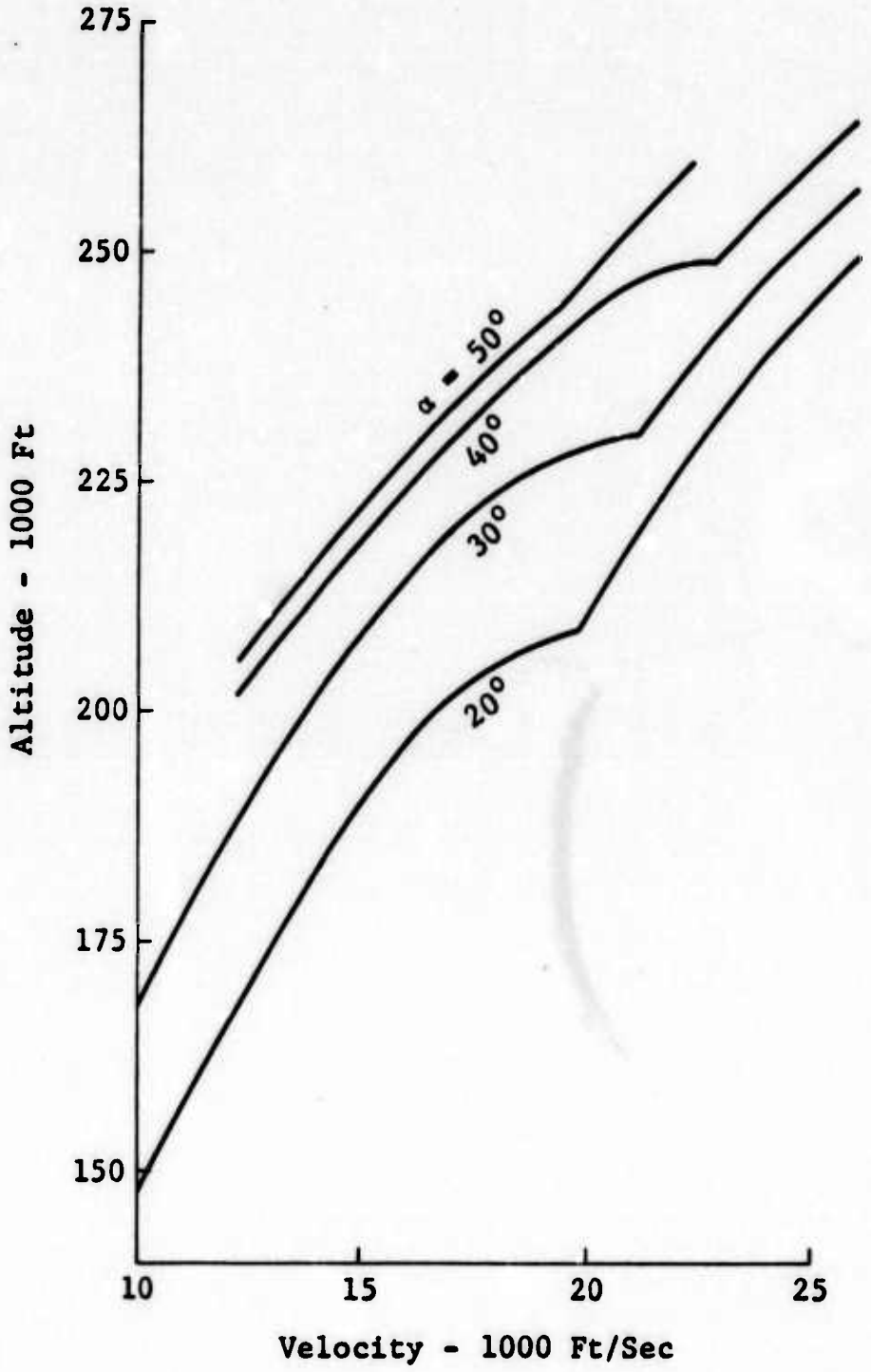

Fig. 3 Thermal Boundary to Maintain Centerline Aft of 20 Foot Station Below 1800°F

VARIATIONAL TREATMENT

Unlike the early energy approximation studies where only one differential equation had to be analyzed, the present investigation involves four differential equations of motion and two inequality constraints on the control and state variables. This more complex problem requires the application of optimal control theory (Ref. 26) to formulate the necessary conditions for a maximum crossrange turning re-entry. These conditions, together with the state equations (11) to (14), form a two-point boundary value problem that must be solved numerically/iteratively for a specific set of boundary conditions.

Necessary Conditions

The Hamiltonian for the unconstrained problem is

$$H = -\lambda_E \frac{DV}{W} + \lambda_\chi \left(\frac{g_o L \sin \mu}{WV} - \frac{V}{r} \sin \chi \tan \varphi\right) - \lambda_\varphi \left(\frac{V}{r} \cos \chi\right) + \lambda_\Lambda \left(\frac{V \sin \chi}{r \cos \varphi}\right) \tag{20}$$

and the augmented Hamiltonian for the constrained problem is

$$\tilde{H} = H + \nu_{UB} C_{UB} + \nu_{ML} C_{ML} \tag{21}$$

where λ_E, λ_χ, λ_φ, λ_Λ are undetermined multipliers, $C_{UB} = h - h_{UB} \geq 0$ is the underbody heating constraint, $C_{ML} = L_{max} - L \geq 0$ is the maximum lift constraint, h_{UB} is given by the thermal boundaries in Fig. 3, L_{max} is the maximum lift with maximum $C_L = 0.535$, and ν_{UB}, ν_{ML} are undetermined constraint multipliers that must satisfy the following conditions

$$\nu_{UB} = 0 \quad \text{if} \quad C_{UB} = h - h_{UB} > 0$$

$$\nu_{UB} \geq 0 \quad \text{if} \quad C_{UB} = h - h_{UB} \leq 0 \tag{22}$$

$$\nu_{MB} = 0 \quad \text{if} \quad C_{ML} = L_{max} - L > 0$$

$$\nu_{MB} \geq 0 \quad \text{if} \quad C_{ML} = L_{max} - L \leq 0 \tag{23}$$

The two additional terms in the augmented Hamiltonian correspond to the treatment of inequality constraints by the technique of Valentine (Refs. 27 and 28).

Substitution of Eqs. (10), (16), (18), (19) into Eqs. (20), (21) and differentiation of $\tilde{H}$ with respect to the four state variables leads to the following Euler equations:

$$\dot{\lambda}_E = \left[3\lambda_E C_{D_o} \frac{\rho S}{2W} V^2 + \lambda_\chi \frac{\sin\chi \tan\varphi}{r} + \lambda_\varphi \frac{\cos\chi}{r} - \lambda_\Lambda \frac{\sin\chi}{r\cos\varphi} \right] \frac{\partial V}{\partial E}$$

$$+ \lambda_E C_{D_{C_L^2}} \frac{2W}{\rho S} \left[\frac{3V^2}{g_o^2 r^2} - \frac{r_o^4}{V^2 r^4} - \frac{2r_o^2}{g_o r^3} \right] \frac{\partial V}{\partial E} \sec^2\mu \tag{24}$$

$$+ \lambda_\chi \left[\frac{g_o r_o^2}{V^2 r^2} + \frac{1}{r} \right] \frac{\partial V}{\partial E} \tan\mu - \nu_{UB} \frac{\partial C_{UB}}{\partial F} - \nu_{ML} \frac{\partial C_{ML}}{\partial E}$$

$$\dot{\lambda}_\chi = \left[\left\{ \lambda_\chi \tan\varphi - \lambda_\Lambda \frac{1}{\cos\varphi} \right\} \cos\chi - \lambda_\varphi \sin\chi \right] \frac{V}{r} \tag{25}$$

$$\dot{\lambda}_\varphi = \left[\lambda_\chi - \lambda_\Lambda \sin\varphi \right] \frac{V}{r} \frac{\sin\chi}{\cos^2\varphi} \tag{26}$$

$$\dot{\lambda}_\Lambda = 0 \quad ; \quad \lambda_\Lambda = \text{constant} \tag{27}$$

where, by differentiating Eq. (9),

$$\frac{\partial V}{\partial E} = \frac{g_o}{V} \tag{28}$$

The partial derivatives $\partial C_{UB}/\partial E$ and $\partial C_{ML}/\partial E$ are given in Appendix C. Since C_{UB} and C_{ML} are not functions of χ, φ, or Λ, their partial derivatives do not appear in Eqs. (25) to (27).

For optimality, the Hamiltonian must be stationary with respect to the two control variables. The Hamiltonian, for the unconstrained case, or unconstrained portion of a trajectory, can be written as

$$H = A + B \sec^2\mu + C \tan \mu \tag{29}$$

where

$$A = - \lambda_E C_{D_o} \frac{\rho S}{2W} V^3 - \lambda_\chi \frac{V}{r} \tan \varphi \sin \chi$$
$$- \lambda_\varphi \frac{V}{r} \cos \chi + \lambda_\Lambda \frac{V \sin \chi}{r \cos \varphi} \tag{30}$$

$$B = - \lambda_E C_{D_{C_L^2}} \frac{2WV}{\rho S g_o^2} \left[\frac{g_o r_o^2}{V r^2} - \frac{V}{r} \right]^2 \tag{31}$$

$$C = \lambda_\chi \left[\frac{g_o r_o^2}{V r^2} - \frac{V}{r} \right] \tag{32}$$

Bank angle is determined by the partial derivative $\partial H/\partial \mu = 0$, and is obtained by differentiating Eq. (29). The result is

$$\tan \mu = - \frac{C}{2B} \tag{33}$$

Substitution of Eq. (33) into Eq. (25) results in

$$H = A + B - \frac{C^2}{4B} \tag{34}$$

which is now a function of only one variable, r. The value of r which minimizes the Hamiltonian [Eq. (34)] is determined by a one dimensional search.

The Hamiltonian as given by Eq. (29) assumes a parabolic drag relationship; however, a similar investigation can be carried out for a fourth-order drag model. The Hamiltonian, Euler equations, and optimum bank angle for this more realistic drag model are given in Appendix D.

For the case involving the underbody heating constraint, the Hamiltonian $\tilde{H}$ must also be stationary with respect to the control variables. This results in

$$\frac{\partial \tilde{H}}{\partial \mu} = \frac{\partial H}{\partial \mu} + \nu_{UB} \frac{\partial C_{UB}}{\partial \mu} = 0 \tag{35}$$

$$\frac{\partial \tilde{H}}{\partial r} = \frac{\partial H}{\partial r} + \nu_{UB} \frac{\partial C_{UB}}{\partial r} = 0 \tag{36}$$

Similarly, for the maximum lift constraint portion of a trajectory

$$\frac{\partial \tilde{H}}{\partial \mu} = \frac{\partial H}{\partial \mu} + \nu_{ML} \frac{\partial C_{ML}}{\partial \mu} = 0 \tag{37}$$

$$\frac{\partial \tilde{H}}{\partial r} = \frac{\partial H}{\partial r} + \nu_{ML} \frac{\partial C_{ML}}{\partial r} = 0 \tag{38}$$

Eq. (41) was used as a check on the accuracy of the numerical procedure. As previously mentioned, the initial conditions of E, χ, φ, Λ, t are specified as well as the final value of E; final values of χ, φ, Λ, t are open. The integration forward in time can proceed once appropriate choices are made for the initial values of the undetermined multipliers. One of these multipliers is selected by the scaling condition, i.e., $\lambda_{E_o} = -1$; a second multiplier can be determined from Eqs. (29) to (32) and (41), which at t_o reduces to

$$\lambda_{\Lambda_o} = \frac{r}{V}\left[\frac{C^2}{4B} - B - C_{D_o}\frac{\rho S V^3}{2W}\right] \tag{42}$$

Since λ_{Λ_o} is a function of r, the Hamiltonian has to be minimized before computing λ_{Λ_o} from Eq. (42). A family of trajectories can be generated in terms of the remaining two multiplier initial values λ_{φ_o} and λ_{χ_o}. A point on the footprint is obtained by selecting λ_{χ_o} and iteratively searching for that value of λ_{φ_o} which results in a solution that satisfies all necessary conditions and for which the final value of λ_{χ_f} is zero (transversality condition). A neighboring point on the footprint is obtained by varying λ_{χ_o} and λ_{φ_o}, utilizing continuity properties of the state and multiplier variables with respect to boundary conditions.

The constraint multipliers for the constrained portion of the trajectory are obtained from Eqs. (36) and (38), resulting in

$$\nu_{UB} = -\frac{\partial H}{\partial r} \Big/ \frac{\partial C_{UB}}{\partial r} \tag{43}$$

$$\nu_{ML} = -\frac{\partial H}{\partial} \Big/ \frac{\partial C_{ML}}{\partial r} \tag{44}$$

For the case where both constraints apply at the same time, Eqs. (39) and (40) are solved simultaneously

$$\begin{bmatrix} \nu_{UB} \\ \nu_{ML} \end{bmatrix} = - \begin{bmatrix} \frac{\partial C_{UB}}{\partial \mu} & \frac{\partial C_{ML}}{\partial \mu} \\ \frac{\partial C_{UB}}{\partial r} & \frac{\partial C_{ML}}{\partial r} \end{bmatrix}^{-1} \begin{bmatrix} \frac{\partial H}{\partial \mu} \\ \frac{\partial H}{\partial r} \end{bmatrix} \tag{45}$$

At each time interval a one dimensional search is made for the altitude that minimizes the Hamiltonian. For each altitude during the search Eqs. (33), (10), (16), and (17) are used to compute the unconstrained optimum bank angle and angle of attack, and the results compared with the heating constraint given by Fig. 3. If the heating constraint is violated the unconstrained numerical results are discarded in favor of the nearest angle of attack that will satisfy the constraint. This is accomplished by the following iterative procedure, initiated with the numerical value of the unconstrained angle of attack:

1. $\Delta\alpha_i = \left(h - h_{UB_{i-1}}\right) \Big/ \frac{\partial h_{UB}}{\partial \alpha}$

2. $\alpha_i = \alpha_{i-1} + \Delta\alpha_i$

3. $h_{UB_i} = h_{UB}(\alpha_i, V)$

4. Test $\left|h - h_{UB_i}\right| < \epsilon$

where ϵ is an arbitrary small number, h_{UB} is a double table look-up with data taken from Fig. 3, and $\partial h_{UB}/\partial\alpha$ is a piecewise-constant function taken from the data stored in the double table

look-up. The four steps are repeated until the altitude difference is less than ϵ. The cosine of the bank angle is then computed from Eqs. (10) and (15) to (17), i.e.,

$$\cos \mu = \frac{WV}{g_o L}\left[\frac{g_o}{V}\left(\frac{r_o}{r}\right)^2 - \frac{V}{r}\right] \tag{46}$$

If $\cos \mu > 1$, an impossible equilibrium flight condition exists for that altitude and the next value of attitude is selected in the search to minimize H. If $\cos \mu > 1$ for all values of altitude, the heating constraint cannot be satisfied and the run is terminated.

The maximum lift coefficient constraint is satisfied by computing lift from Eq. (10), maximum lift from Eq. (16) using $C_L = C_{L_{max}}$, and verifying that $L < L_{max}$. If $L > L_{max}$, the unconstrained values of bank angle and angle of attack are discarded and, instead, Eq. (46) is used to compute the constrained bank angle with $L = L_{max}$, and, the search is continued for the value of r that minimizes H.

NUMERICAL RESULTS

The numerical data employed for the re-entry vehicle corresponds to one of the early (1970) space shuttle orbiter configurations. A FORTRAN IV digital computer program was used to calculate iteratively both unconstrained and constrained optimum trajectories. The footprints for both are shown in Fig. 4 as a locus of terminal latitudinal and longitudinal points for a fixed terminal energy state. The unconstrained footprint was traced from the easily determined maximum downrange point ($\varphi = \chi = \mu = \lambda_\varphi = \lambda_\chi = 0$), back along the north branch and past the maximum crossrange point. No attempt was made to define the rear of the footprint, which is believed to involve zigzagging paths. The effect of the heating constraint is to shrink the footprint, as would be expected, with the maximum downrange and crossrange reduced by 64 and 450 nautical miles, respectively.

Figures 5, 6, and 7 show the trajectory characteristics for typical high and low crossrange solutions, with and without heating constraints. For the sequence of runs that include the heating constraint, the trajectories are initially constrained, remain so most of the time, and thereafter continue to be unconstrained.

The high sensitivity of the final state conditions with respect to the initial conditions of the multipliers is demonstrated in Fig. 8. Optimal runs have zero bank at the terminal conditions. This can be shown by substituting Eqs. (31) and (32) into Eq. (33)

$$\tan \mu = \frac{\lambda_\chi \rho S g_o^2}{4\lambda_E W C_D C_L^2 \left[\frac{g_o r_o^2}{r^2} - \frac{V^2}{r}\right]} \tag{47}$$

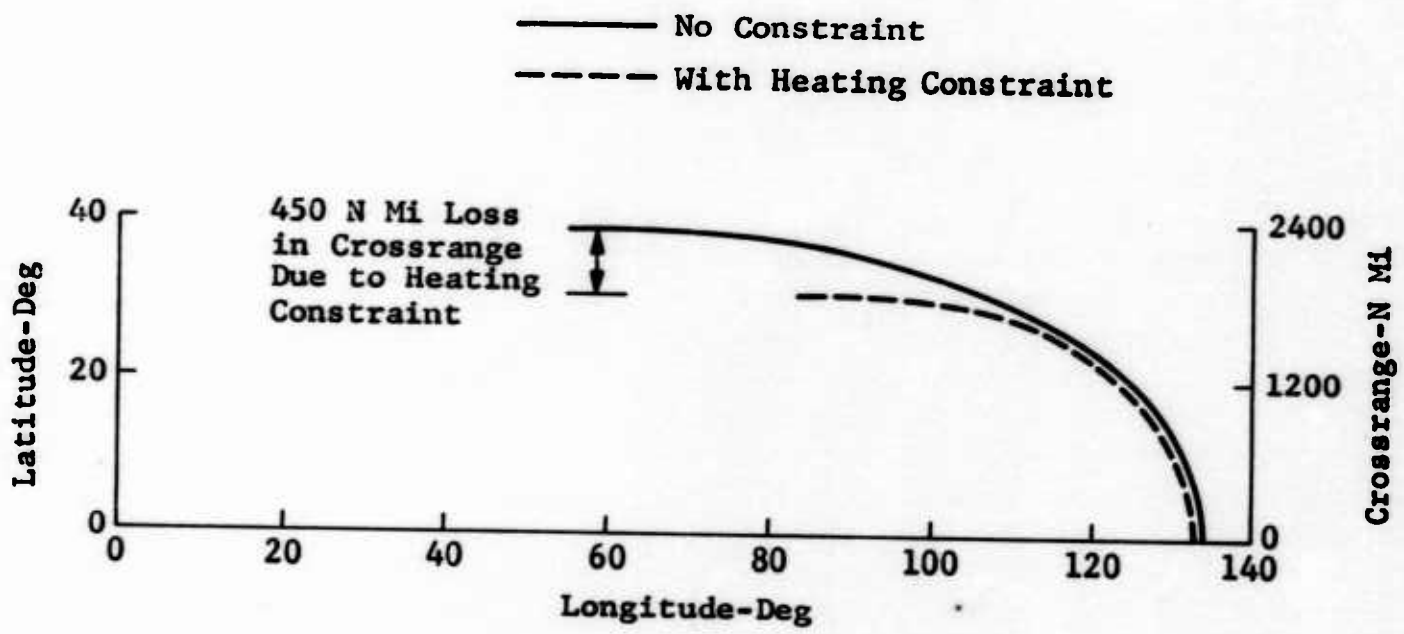

Fig. 4 Landing Footprints for Space Shuttle Re-entry Using Reduced-Order Approximation

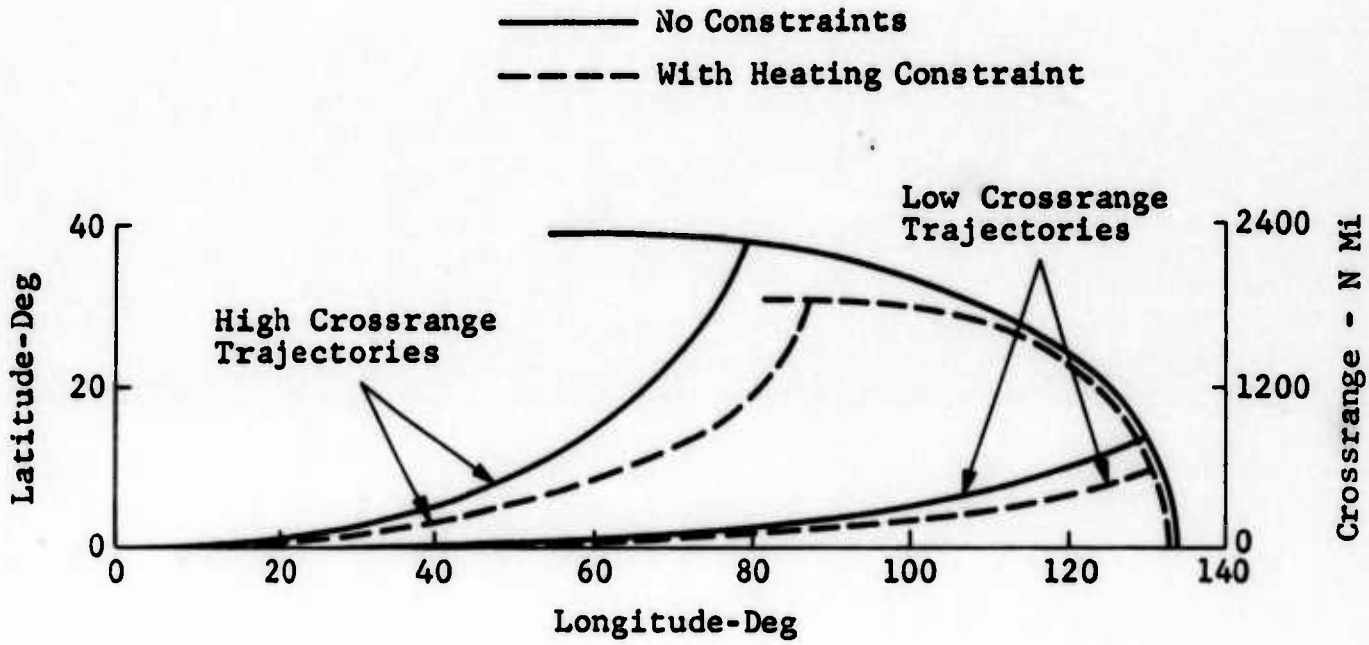

Fig. 5 Typical Reduced-Order Trajectories for Space Shuttle Re-entry - Latitude vs Longitude

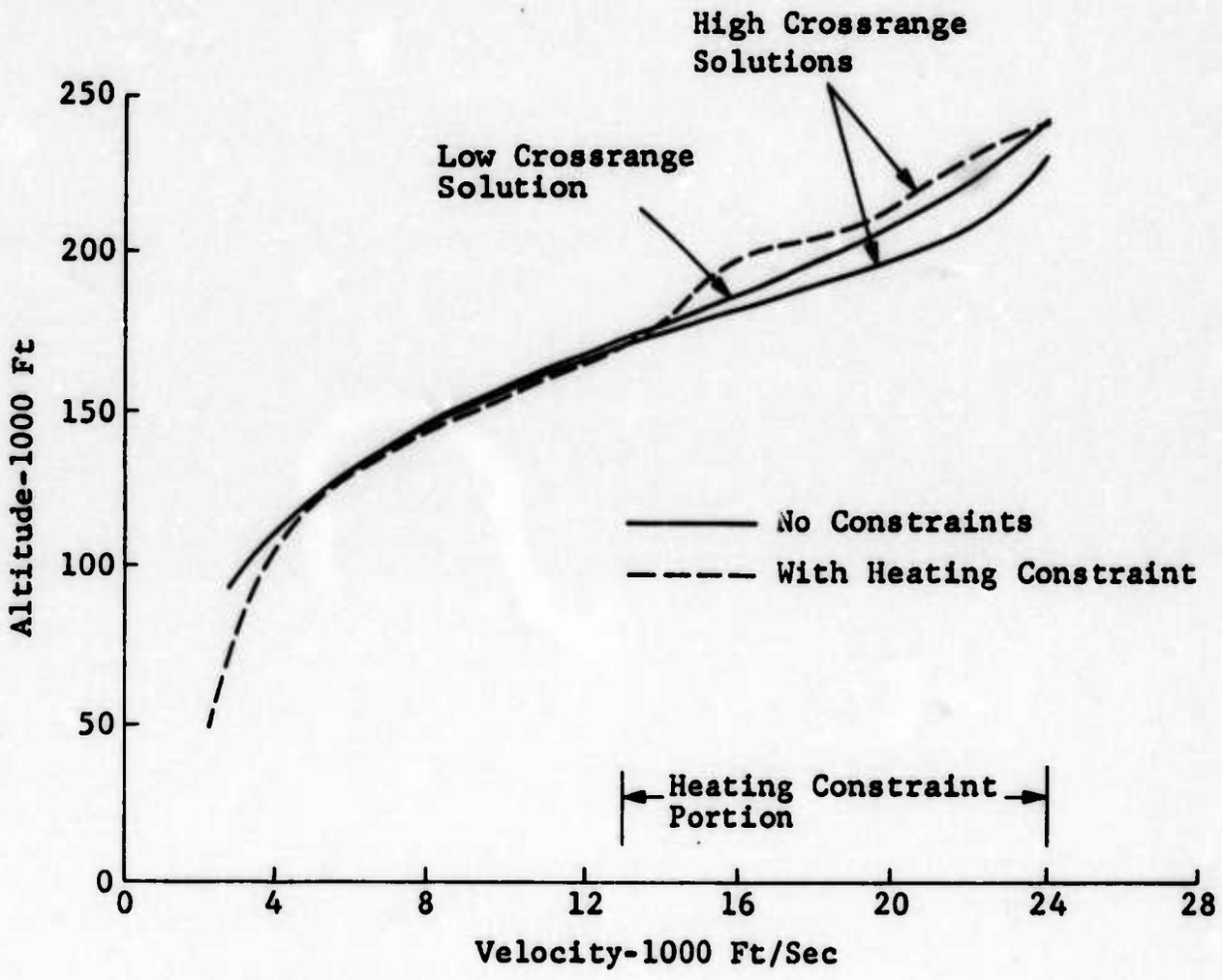

Fig. 6 Typical Reduced-Order Solutions for Space Shuttle Re-entry - Altitude vs Velocity

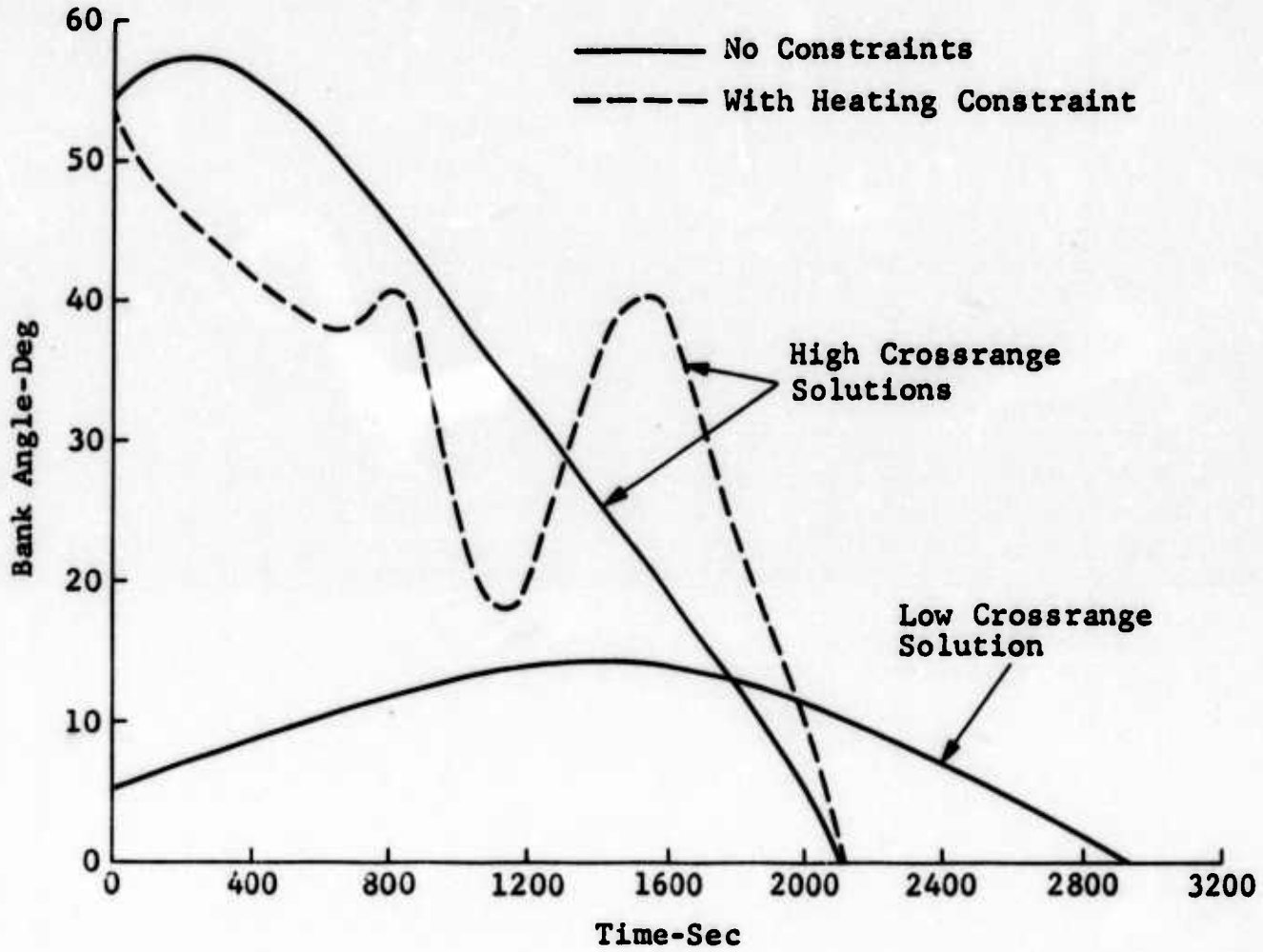

Fig. 7 Typical Bank Angle Time Histories for Reduced-Order Solutions

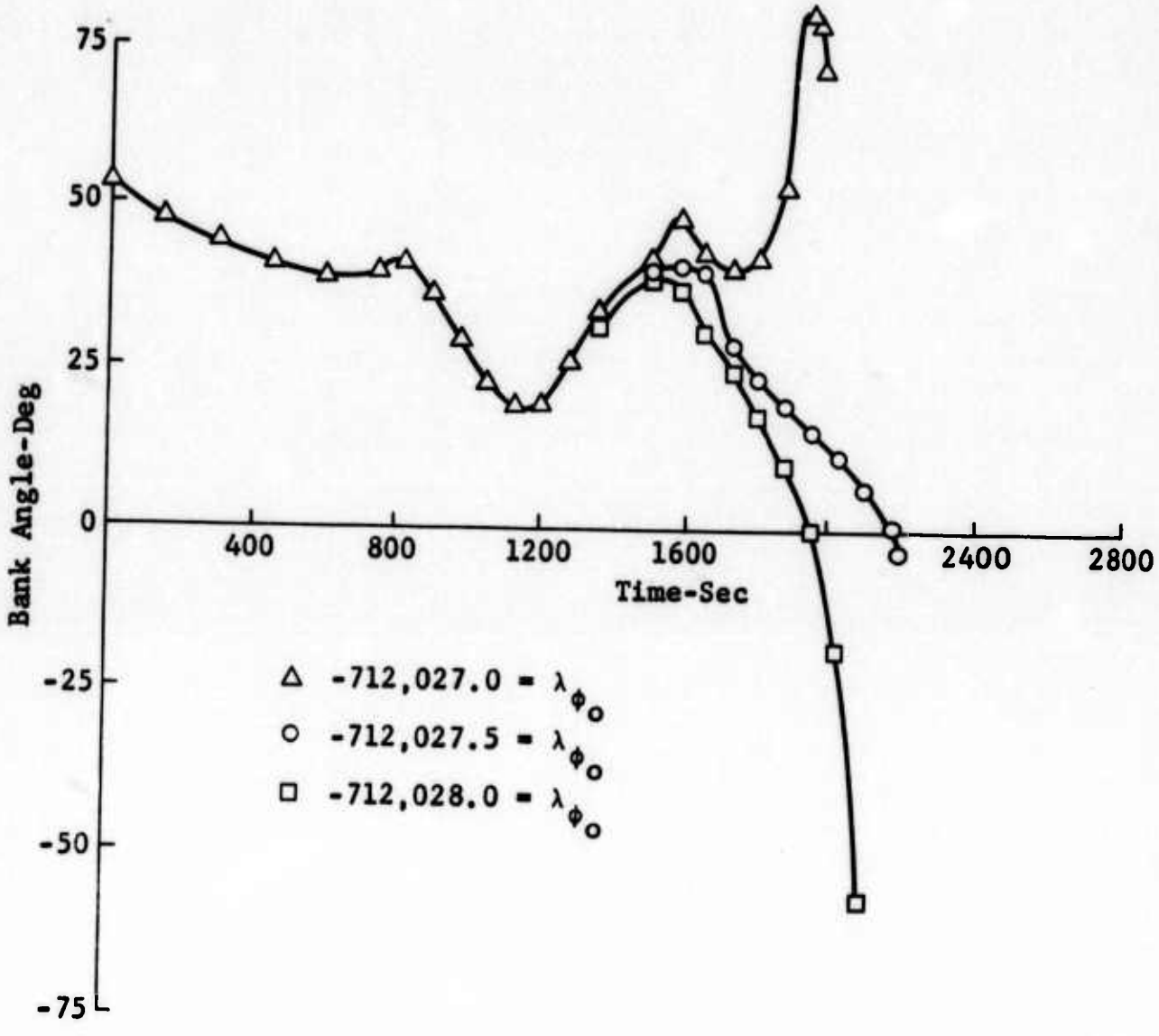

Fig. 8 Example of High Sensitivity of Terminal Control Variations to Small Changes in the Initial λ_ϕ Multiplier

and noting that the transversality condition calls for $\lambda_{\chi_f} = 0$. Neighboring solutions have hard right or hard left maneuvers depending upon the sign of λ_χ at the specified value of $E_f = -20{,}800{,}000$ feet. Fortunately, in spite of this sensitivity, it is clear-cut how to change iteratively the numerical value of λ_{φ_o} to achieve $\lambda_{\chi_f} = 0$.

The maximum lift constraint was added to the computer program in the anticipation that large bank angles at high altitudes, or high altitudes resulting from the heating constraint, would call for excessive lift capability. However, this never occurred. Instead, it was noted that the lift constraint was necessary at the end of some of those trajectories that involved hard turning maneuvers. For those trajectories with $\lambda_{\chi_f} = 0$, i.e., $\mu_f = 0$, the lift constraint was never required.

In Appendix B it is shown analytically that the optimum angle of attack for the unconstrained case, or unconstrained portion of a trajectory, is that which maximizes L/D. Substitution of the numerical data into Eqs. (B-22) and (17) produces an angle of attack of $15.6°$. No attempt was made to capitalize on this analytical result when writing the computer program; however, all of the numerical solutions for the unconstrained cases, as well as the unconstrained portions of the constrained cases (see Fig. 9), consist of angle of attack time histories that remains constant at $15.6°$, thus verifying the analytical finding. It has been shown in the classical literature that for two dimensional flight over a flat earth maximum L/D will provide the most range. The analytic solution of Appendix B and all of the numerical results of this report (without constraints) show that maximum L/D is also the optimum control that maximizes range and crossrange for three dimensional turning flight over a spherical earth with an inverse-square gravity field.

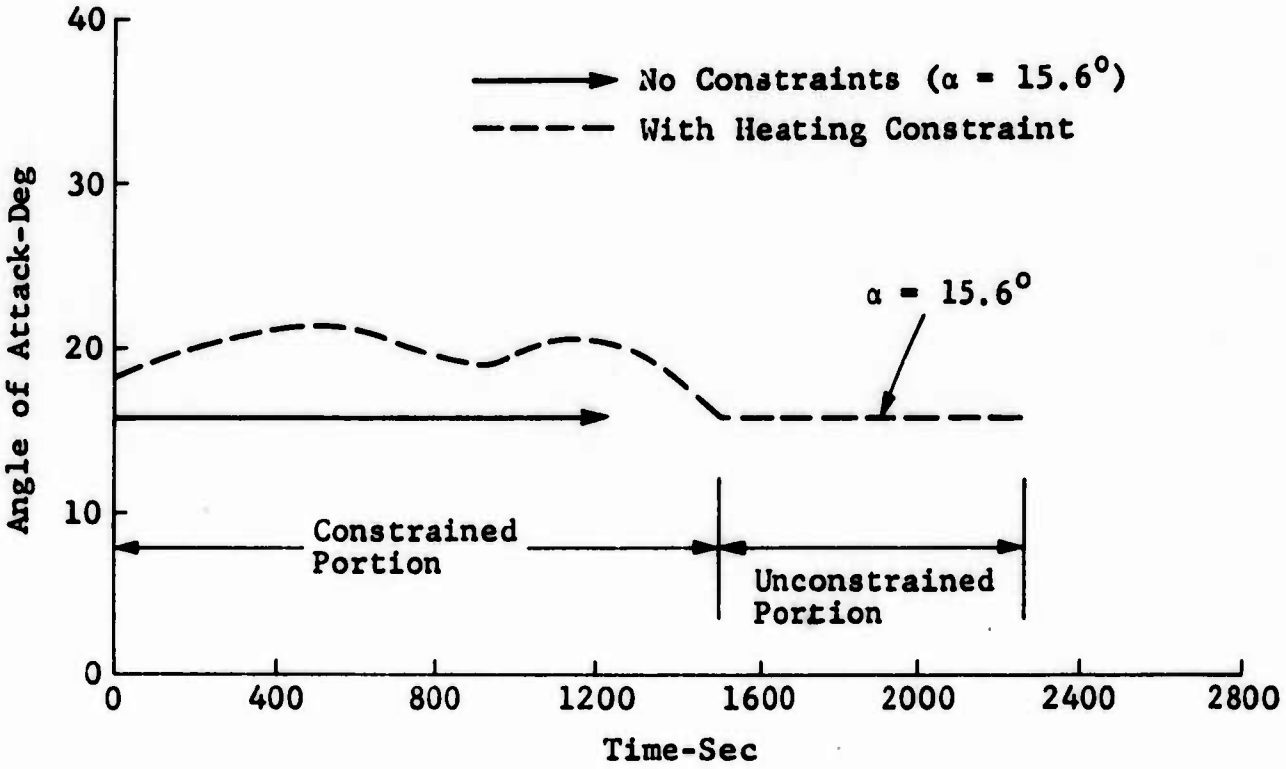

Fig. 9 Typical Angle of Attack Time Histories for Reduced-Order Solutions

Throughout the investigation and computer programming no deliberate effort was made to minimize machine time. However, there are several worthwhile approaches that could be exploited. The first is to take advantage of the analytic solution, maximum L/D angle of attack, for the unconstrained re-entry and unconstrained portions of the trajectories. The optimal controls are given explicitly in Appendix B by Eqs. (B-22) and (B-24). No numerical search is necessary to minimize the Hamiltonian; however, a simple iterative procedure may be required to determine the altitude from Eq. (B-7). The second approach at streamlining the computer program would be to utilize the constants of motion from Noether's theorem (Appendix E), together with the constant, zero value of the Hamiltonian. These four constants, given by Eqs. (C-1), (C-2), (C-3), and (41), eliminate the need to numerically integrate Eqs. (24) to (26). A third approach would be to utilize a system of differential equations where energy is used as the independent variable (Appendix B). This would eliminate the need to numerically integrate Eq. (11). Although the Hamiltonian would no longer be constant, this would be compensated by the elimination of the energy multiplier, λ_E.

APPENDIX A

DERIVATION OF EQUATIONS OF MOTION

The flight path equations of motion could be derived from first principles; however, a rigorous development would be rather lengthy and not in keeping with the purpose of this report. Instead, utilization will be made of Ref. 29 which provides a thorough derivation and requires only a few additional substitutions to obtain Eqs. (1) to (6). Since many of the variables of Ref. 29 have definitions and symbols different from those of this report, only Appendix A will employ the symbols of Ref. 29.

The curvilinear coordinates X and Y are related to longitude τ and latitude λ (Fig. A-1) by simple arc length formulae given by Eqs. (6) on p. 61 of Ref. 29

$$X = r_o \tau \quad , \quad Y = r_o \lambda \tag{A-1}$$

where the constant r_o is the radius of the earth. The resulting curvilinear velocities are

$$\dot{X} = r_o \dot{\tau} \quad , \quad \dot{Y} = r_o \dot{\lambda} \tag{A-2}$$

The angular velocities of the wind axes (p_w, q_w, r_w) centered at the vehicle's cg (Fig. A-2) are related to earth fixed axes centered at some point on the surface of the earth (Fig. A-1) by Eq. (17) on p. 63. Substitution of (A-1) and (A-2) into this equation results in

$$\begin{bmatrix} p_w \\ q_w \\ r_w \end{bmatrix} = \begin{bmatrix} 1 & 0 & -\sin\gamma \\ 0 & \cos\mu & \sin\mu\cos\gamma \\ 0 & -\sin\mu & \cos\mu\cos\gamma \end{bmatrix} \begin{bmatrix} \dot{\mu} \\ \dot{\gamma} \\ \dot{\chi} \end{bmatrix} +$$

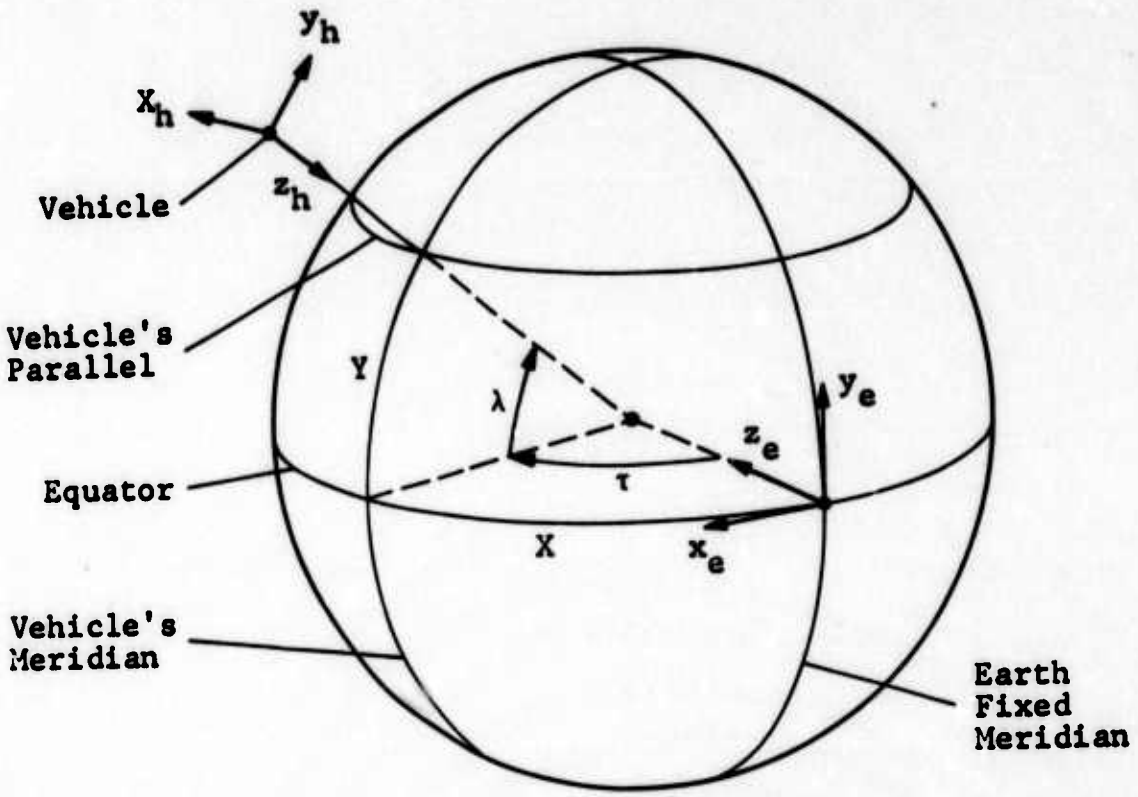

Fig. A-1 Coordinate Systems for Flight Over Spherical Earth (Ref. 29)

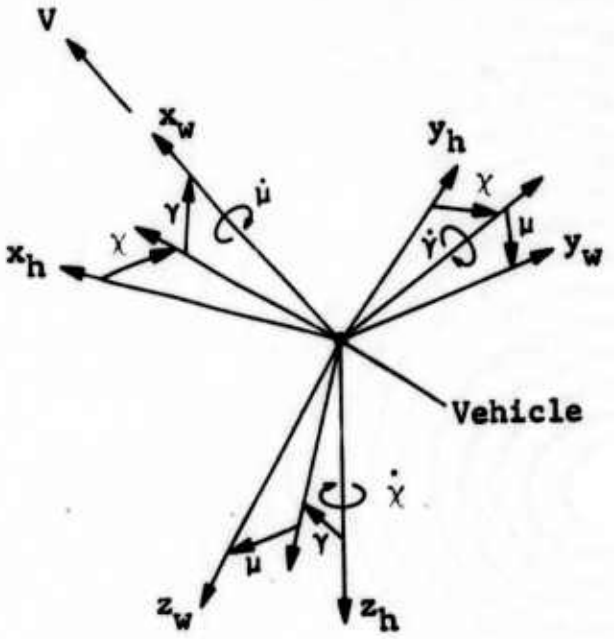

Fig. A-2 System of Rotations from Local Horizon to Wind Axes (Ref. 29)

$$\begin{bmatrix} \cos\gamma\cos\chi & \cos\gamma\sin\chi & -\sin\gamma \\ \sin\mu\sin\gamma\cos\chi - \cos\mu\sin\chi & \sin\mu\sin\gamma\sin\chi + \cos\mu\cos\chi & \sin\mu\cos\gamma \\ \cos\mu\sin\gamma\cos\chi + \sin\mu\sin\chi & \cos\mu\sin\gamma\sin\chi - \sin\mu\cos\chi & \cos\mu\cos\gamma \end{bmatrix} \begin{bmatrix} \dot{\lambda} \\ -\dot{\tau}\cos\lambda \\ \dot{\tau}\sin\lambda \end{bmatrix} \quad \text{(A-3)}$$

where χ is the azimuth heading angle (0° due west, 90° due north, etc.), γ is the flight path angle above horizontal, and μ is the bank angle (positive right wing down). The kinematic relationships, which when integrated defines the vehicle's position with respect to the earth, are given by Eqs. (22) on p. 64. Substitution of (A-1) and (A-2) into this equation results in

$$\dot{\tau} = \frac{V}{r}\frac{\cos\gamma\cos\chi}{\cos\lambda} \quad \text{(A-4)}$$

$$\dot{\lambda} = \frac{V}{r}\cos\gamma\sin\chi \quad \text{(A-5)}$$

$$\dot{h} = V\sin\gamma \quad \text{(A-6)}$$

where h is the altitude and $r = r_o + h$ is the distance of the vehicle from the center of the earth. Gravity, the usual inverse-square law, is given by Eq. (25) on p. 65

$$g = g_o\left(\frac{r_o}{r_o + h}\right)^2 \quad \text{(A-7)}$$

The dynamical relationships are given by Eqs. (26) on p. 65. Substitution of (A-7) into this equation and assuming no thrust, a coordinated turn with no side force, and a nonrotating earth results in

$$\dot{V} = -(D/m) - g \sin \gamma \tag{A-8}$$

$$r_w = (g/V)\sin \mu \cos \gamma \tag{A-9}$$

$$q_w = (L/mV) - (g/V)\cos \mu \cos \gamma \tag{A-10}$$

Substitution of r_w and q_w from (A-3) into (A-9) and (A-10) becomes

$$\dot{\chi} \cos \mu \cos \gamma - \dot{\gamma} \sin \mu + (V/r)\cos \gamma \sin \mu + (V/r)\cos^2\gamma \cos \chi \cos \mu \tan \lambda = (g/V)\sin \mu \cos \gamma \tag{A-11}$$

$$\dot{\chi} \sin \mu \cos \gamma + \dot{\gamma} \cos \mu - (V/r)\cos \gamma \cos \mu + (V/r)\cos^2\gamma \cos \chi \sin \mu \tan \lambda = (L/mV) - (g/V)\cos \mu \cos \gamma \tag{A-12}$$

Multiplying (A-11) by $\cos \mu$ and (A-12) by $\sin \mu$ and then adding, and similarly multiplying (A-11) by $-\sin \mu$ and (A-12) by $\cos \mu$ and then adding, results in

$$\dot{\chi} \cos \gamma + (V/r)\cos^2\gamma \cos \chi \tan \lambda = (L/mV)\sin \mu \tag{A-13}$$

$$\dot{\gamma} - (V/r)\cos \gamma = (L/mV)\cos \mu - (g/V)\cos \gamma \tag{A-14}$$

The six degree of freedom equations are composed of (A-4), (A-5), (A-6), (A-8), (A-13), and (A-14). Since $\dot{h} = \dot{r}$, these equations can be summarized as:

$$\dot{V} = -\frac{D}{m} - g \sin \gamma \tag{A-15}$$

$$\dot{\gamma} = \frac{L}{mV} \cos \mu - \frac{g}{V} \cos \gamma + \frac{V}{r} \cos \gamma \tag{A-16}$$

$$\dot{\chi} = \frac{L \sin \mu}{mV \cos \gamma} - \frac{V}{r} \cos \gamma \cos \chi \tan \lambda \tag{A-17}$$

$$\dot{r} = V \sin \gamma \tag{A-18}$$

$$\dot{\tau} = \frac{V}{r} \frac{\cos \gamma \cos \chi}{\cos \lambda} \tag{A-19}$$

$$\dot{\lambda} = \frac{V}{r} \cos \gamma \sin \chi \tag{A-20}$$

The differences between the above six equations and Eqs. (1) to (6) are due to differences in definitions and symbols. The longitude τ increases heading west (Fig. A-1), whereas Λ in (6) increases heading east; the bank angle μ above is positive right wing down, whereas in (2) and (3) it is positive left wing down; and the azimuth heading angle in (3), (5), and (6) is $0°$ due south, $90°$ due east, etc. If the following four changes are made, Eqs. (1) to (6) will be obtained

$$\tau \rightarrow -\Lambda \quad , \quad \mu \rightarrow -\mu$$

$$\lambda \rightarrow \varphi \quad , \quad \chi \rightarrow 270° - \chi$$

An almost identical system of equations of motion can also be found in Ref. 30.

APPENDIX B

CHANGE OF INDEPENDENT VARIABLE FROM TIME TO ENERGY

Based on the somewhat limited numerical results of this report it is possible to convert the independent variable from time to velocity, or heading angle, or latitude, or longitude, since all of these state variables have been noted to vary monotonically for the reduced-order solutions. However, energy is the only state variable which is certain always to vary monotonically for all unpowered flight problems, even for the complete six degree of freedom equations. From Eqs. (11) and (1) to (6)

$$\frac{dt}{dE} = -\frac{W}{DV} \tag{B-1}$$

$$\frac{d\gamma}{dE} = \frac{d\gamma}{dt}\frac{dt}{dE} = -\frac{Lg_o}{DV^2}\cos\mu + \frac{Wg}{DV^2}\cos\gamma - \frac{W}{Dr}\cos\gamma \tag{B-2}$$

$$\frac{d\chi}{dE} = \frac{d\chi}{dt}\frac{dt}{dE} = -\frac{Lg_o}{DV^2}\frac{\sin\mu}{\cos\gamma} + \frac{W}{Dr}\cos\gamma\sin\chi\tan\varphi \tag{B-3}$$

$$\frac{dr}{dE} = \frac{dr}{dt}\frac{dt}{dE} = -\frac{W}{D}\sin\gamma \tag{B-4}$$

$$\frac{d\varphi}{dE} = \frac{d\varphi}{dt}\frac{dt}{dE} = \frac{W}{Dr}\cos\gamma\cos\chi \tag{B-5}$$

$$\frac{d\Lambda}{dE} = \frac{d\Lambda}{dt}\frac{dt}{dE} = -\frac{W}{Dr}\frac{\cos\gamma\sin\chi}{\cos\varphi} \tag{B-6}$$

Utilizing the same previous assumptions, that the flight path angle γ is small and the angular rate $\dot{\gamma}$ is zero, (B-2) and (B-4) are converted to algebraic expressions

$$\frac{W}{D} = \frac{L}{D} \frac{g_o r}{(gr - V^2)} \cos \mu \tag{B-7}$$

$$r = r_o + h \tag{B-8}$$

The system of differential equations is reduced to third order:

$$\frac{d\gamma}{dE} = \frac{L}{D}\left[\frac{g_o}{(gr - V^2)} \cos \mu \sin \gamma \tan \varphi - \frac{g_o}{V^2} \sin \mu\right] \tag{B-9}$$

$$\frac{d\varphi}{dE} = \frac{L}{D} \frac{g_o}{(gr - V^2)} \cos \mu \cos \gamma \tag{B-10}$$

$$\frac{d\Lambda}{dE} = - \frac{L}{D} \frac{g_o}{(gr - V^2)} \frac{\cos \mu \sin \gamma}{\cos \varphi} \tag{B-11}$$

The coefficients involving gravity and velocity are converted with the use of the energy equation (9)

$$\frac{g_o}{(gr - V^2)} = \frac{-1}{2E + \frac{r_o^2}{r}} \tag{B-12}$$

$$\frac{g_o}{V^2} = \frac{1}{2\left(E + \frac{r_o^2}{r}\right)} \tag{B-13}$$

Equations (B-9) to (B-11) become

$$\frac{d\gamma}{dE} = \frac{L}{D}\left[- \frac{\cos \mu}{2E + \frac{r_o^2}{r}} \sin \gamma \tan \varphi - \frac{\sin \mu}{2\left(E + \frac{r_o^2}{r}\right)}\right] \tag{B-14}$$

$$\frac{d\varphi}{dE} = -\frac{L}{D}\frac{\cos\mu}{2E + \frac{r_o^2}{r}}\cos\chi \tag{B-15}$$

$$\frac{d\Lambda}{dE} = \frac{L}{D}\frac{\cos\mu}{2E + \frac{r_o^2}{r}}\frac{\sin\chi}{\cos\varphi} \tag{B-16}$$

and the Hamiltonian can be written:

$$H = \frac{L}{D}\left[\frac{\cos\mu}{2E + \frac{r_o^2}{r}}\left(\frac{\sin\chi}{\cos\varphi}\left\{\lambda_\Lambda - \lambda_\chi \sin\varphi\right\} - \lambda_\varphi\cos\chi\right)\right. \tag{B-17}$$

$$\left. - \frac{\sin\mu}{2\left(E + \frac{r_o^2}{r}\right)}(\lambda_\chi)\right]$$

Although there are three control variables in (B-17), namely r, μ, and α (L/D is a function only of α), r plays a very insignificant part, almost like a constant. This is vastly different from the Hamiltonian given by Eqs. (29) to (32), where the air density ρ, which is strongly dependent on r, appears in the A and B terms. For example, at a typical initial condition of $V = 24{,}100$ ft/sec and $h = 233{,}000$ ft, a rather large change in r of 10,000 ft results in a 52% change in ρ and only a 0.38% change in $(2E + r_o^2/r)$ and a 0.11% change in $2(E + r_o^2/r)$. Advantage can be taken of this property by employing the following different procedure for minimizing the Hamiltonian while satisfying the $\dot{\gamma} = 0$ condition, i.e., (B-7).

Equation (B-17) can also be written as

$$H = \frac{L}{D}[A \cos \mu + B \sin \mu] \tag{B-18}$$

where

$$A = \frac{1}{2E + \frac{r_o^2}{r}} \left(\frac{\sin \chi}{\cos \varphi} \left\{ \lambda_\Lambda - \lambda_\chi \sin \varphi \right\} - \lambda_\varphi \cos \chi \right) \tag{B-19}$$

$$B = - \frac{\lambda_\chi}{2\left(E + \frac{r_o^2}{r}\right)} \tag{B-20}$$

First, a reasonable guess for r would be made; e.g., the value of r from the previous integration interval. Then the Hamiltonian is minimized with respect to α, which results in maximizing L/D. For drag polars, as given by Eq. (18), it can be shown that

$$\text{Max } L/D = \tfrac{1}{2} \left(C_{D_o} \; C_{D_{C_L^2}} \right)^{-\frac{1}{2}} \tag{B-21}$$

$$C_L(\text{Max } L/D) = \left(C_{D_o} \Big/ C_{D_{C_L^2}} \right)^{\frac{1}{2}} \tag{B-22}$$

The Hamiltonian is then minimized with respect to μ

$$\frac{\partial H}{\partial \mu} = \frac{L}{D}[- A \sin \mu + B \cos \mu] = 0 \tag{B-23}$$

Consequently

$$\tan \mu = \frac{B}{A} \tag{B-24}$$

The $\dot{\gamma} = 0$ condition is then satisfied by iteratively computing a new value of r from (B-7). This procedure of computing A, B, μ, and r can be repeated, if necessary, until the change of r is less than some small specified value.

APPENDIX C

DERIVATION OF PARTIAL DERIVATIVES

The partial derivatives of the augmented Hamiltonian $\tilde{H}$ with respect to the four state variables E, χ, φ, Λ are easily derived and result in the four Euler equations, (24) to (27). All of the other derivatives required for the computer program are obtained by partial differentiation of H, C_{UB}, C_{ML} with respect to E, R, μ. Rules of partial differentiation, concerning which quantites are fixed or variable, are the same as those governing the development of the Euler equations.

$\partial(C_{UB}, C_{ML})/\partial E$

Partial derivatives taken with respect to E are carried out for fixed values of the control variables r, μ, and the state variables χ, φ, Λ. All other variables, such as V, α, C_L, L, etc., are not fixed. Repeating Eq. (22),

$$C_{UB} = h - h_{UB} \tag{C-1}$$

where $h = r - r_o$, and h_{UB} is given by the thermal boundaries in Fig. 3. Differentiating (C-1) with respect to E,

$$\frac{\partial C_{UB}}{\partial E} = - \frac{\partial h_{UB}}{\partial V} \frac{\partial V}{\partial E} - \frac{\partial h_{UB}}{\partial \alpha} \frac{\partial \alpha}{\partial C_L} \frac{\partial C_L}{\partial V} \frac{\partial V}{\partial E} \tag{C-2}$$

where $\partial h_{UB}/\partial V$ and $\partial h_{UB}/\partial \alpha$ are piecewise constant functions computed from h_{UB} data stored in the double table look-up. From the energy equation (9),

$$\frac{\partial V}{\partial E} = \frac{g_o}{V} \tag{C-3}$$

From the angle of attack equation (17),

$$\frac{\partial \alpha}{\partial C_L} = .98 \sec^2(1.33\ C_L) \tag{C-4}$$

Combining Eqs. (10) and (16), and differentiating,

$$C_L = \frac{2W}{\rho S g_o \cos \mu}\left[\frac{g_o r_o^2}{V^2 r^2} - \frac{1}{r}\right] \tag{C-5}$$

$$\frac{\partial C_L}{\partial V} = -\frac{4W r_o^2}{\rho S V^3 r^2 \cos \mu} \tag{C-6}$$

Repeating Eq. (23),

$$C_{ML} = L_{max} - L \tag{C-7}$$

where L_{max} and L are obtained from Eqs. (10) and (16)

$$L_{max} = \tfrac{1}{2} C_{L_{max}} \rho V^2 S \tag{C-8}$$

$$L = \frac{W}{g_o \cos \mu}\left[\frac{g_o r_o^2}{r^2} - \frac{V^2}{r}\right] \tag{C-9}$$

Differentiating (C-7) to (C-9) with respect to E,

$$\frac{\partial C_{ML}}{\partial E} = \frac{\partial L_{max}}{\partial V}\frac{\partial V}{\partial E} - \frac{\partial L}{\partial V}\frac{\partial V}{\partial E} \tag{C-10}$$

$$\frac{\partial L_{max}}{\partial V} = C_{L_{max}} \rho V S \tag{C-11}$$

$$\frac{\partial L}{\partial V} = -\frac{2WV}{g_o r \cos \mu} \tag{C-12}$$

$\partial(H, C_{UB}, C_{ML})/\partial r$

Partial derivatives taken with respect to r are carried out for fixed values of the multipliers, the state variables E, χ, φ, Λ, and the control variable μ. All other variables, such as V, α, C_L, L, etc., are not fixed. The Hamiltonian is given by Eq. (29)

$$H = A + B \sec^2\mu + C \tan \mu \tag{C-13}$$

where A, B, C are given by Eqs. (30) to (32). Differentiating (C-13) with respect to r,

$$\frac{\partial H}{\partial r} = \frac{\partial A}{\partial r} + \frac{\partial B}{\partial r} \sec^2\mu + \frac{\partial C}{\partial r} \tan \mu \tag{C-14}$$

Since A, B, C, as well as C_L, L_{max}, L that follow, are functions of r and V, the partial derivatives are derived by

$$\frac{\partial A}{\partial r} = \left(\frac{\partial A}{\partial r}\right)_V + \left(\frac{\partial A}{\partial V}\right)_r \frac{\partial V}{\partial r} \tag{C-15}$$

where the subscripts indicate which variables are fixed. From Eqs. (9) and (15)

$$\frac{\partial V}{\partial r} = - \frac{g_o r_o^2}{V r^2} \tag{C-16}$$

$$\frac{\partial \rho}{\partial r} = - \beta\rho \tag{C-17}$$

Thus,

$$\frac{\partial A}{\partial r} = \lambda_E C_{D_o} \frac{\rho S V}{2W}\left[\frac{3 g_o r_o^2}{r^2} + \beta V^2\right] + \left[\frac{g_o r_o^2}{V r^3} + \frac{V}{r^2}\right]\left[\lambda_\chi \tan \varphi \sin \chi + \lambda_\varphi \cos \chi - \lambda_\Lambda \frac{\sin \chi}{\cos \varphi}\right] \tag{C-18}$$

$$\frac{\partial B}{\partial r} = -\lambda_E C_D \frac{2W}{\rho S g_o} \left[\beta \left(\frac{g_o^2 r_o^4}{V r^4} - \frac{2V g_o r_o^2}{r^3} + \frac{V^3}{r^2} \right) + \frac{g_o^3 r_o^6}{V^3 r^6} \right. \tag{C-19}$$

$$\left. - \frac{2 g_o^2 r_o^4}{V r^5} + \frac{3V g_o r_o^2}{r^4} - \frac{2V^3}{r^3} \right]$$

$$\frac{\partial C}{\partial r} = \lambda_\chi \left[\frac{g_o r_o^2}{V r^3} \left(\frac{g_o r_o^2}{V^2 r} - 1 \right) + \frac{V}{r^2} \right] \tag{C-20}$$

The derivative $\partial C_{UB}/\partial r$ is obtained by differentiating Eq. (C-1)

$$\frac{\partial C_{UB}}{\partial r} = 1 - \frac{\partial h_{UB}}{\partial V} \frac{\partial V}{\partial r} - \frac{\partial h_{UB}}{\partial \alpha} \frac{\partial \alpha}{\partial C_L} \frac{\partial C_L}{\partial r} \tag{C-21}$$

where, by differentiating Eq. (C-5)

$$\frac{\partial C_L}{\partial r} = \frac{2W}{\rho S g_o \cos \mu} \left[\frac{2 g_o r_o^2 \left(g_o r_o^2 - V^2 r \right)}{V^4 r^4} + \frac{1}{r^2} + \beta \left(\frac{g_o r_o^2}{V^2 r^2} - \frac{1}{r} \right) \right] \tag{C-22}$$

All other derivatives in (C-21) have been previously defined.

The derivative $\partial C_{ML}/\partial r$ is obtained from Eq. (C-7)

$$\frac{\partial C_{ML}}{\partial r} = \frac{\partial L_{max}}{\partial r} - \frac{\partial L}{\partial r} \tag{C-23}$$

where, by differentiating Eqs. (C-8) and (C-9)

$$\frac{\partial L_{max}}{\partial r} = -\tfrac{1}{2} \rho S C_{L_{max}} \left[\frac{2 g_o r_o^2}{r^2} + \beta V^2 \right] \tag{C-24}$$

$$\frac{\partial L}{\partial r} = \frac{WV^2}{g_o r^2 \cos \mu} \tag{C-25}$$

$\partial(H, C_{UB}, C_{ML})/\partial\mu$

Partial derivatives taken with respect to μ are carried out for fixed values of the multipliers, the state variables E, χ, Φ, Λ, and the control variable r. Since V is a function only of E and r, both of which are fixed, V also is fixed. All other variables, such as α, C_L, L, etc., are not fixed. Differentiating Eq. (C-13) with respect to μ,

$$\frac{\partial H}{\partial \mu} = [2B \tan \mu + C]\sec^2\mu \tag{C-26}$$

Differentiating Eq. (C-1) with respect to μ

$$\frac{\partial C_{UB}}{\partial \mu} = - \frac{\partial h_{UB}}{\partial \alpha} \frac{\partial \alpha}{\partial C_L} \frac{\partial C_L}{\partial \mu} \tag{C-27}$$

where the first two derivatives have been previously defined and, by differentiating Eq. (C-5)

$$\frac{\partial C_L}{\partial \mu} = \frac{2W}{\rho S g_o}\left[\frac{g_o r_o^2}{V^2 r^2} - \frac{1}{r}\right][\tan \mu \sec \mu] \tag{C-28}$$

Combining Eqs. (C-7) to (C-9) and differentiating with respect to μ results in

$$\frac{\partial C_{ML}}{\partial \mu} = \frac{W}{g_o}\left[\frac{V^2}{r} - \frac{g_o r_o^2}{r^2}\right]\tan \mu \sec \mu \tag{C-29}$$

APPENDIX D

DRAG POLARS OF FOURTH ORDER

The mathematical formulation and computer program described in this report applies only to those cases where the aerodynamic data are represented by parabolic drag relationships, as given by Eq. (18). Because of the uncertainty in the aerodynamic data, particularly during the preliminary design phase, this simple drag polar should be adequate for many studies. However, as more wind tunnel data become available, it may be necessary to improve the polar curve fit by adding a fourth-order term

$$C_D = C_{D_o} + C_{D_{C_L^2}} C_L^2 + C_{D_{C_L^4}} C_L^4 \qquad \text{(D-1)}$$

where $C_{D_{C_L^4}}$ is always positive, both for straight and swept wing re-entry vehicles. In the following analysis, this is not only important, but fortunate. For this fourth-order drag polar, the Hamiltonian is

$$H = A + B \sec^2\mu + C \tan\mu + F \sec^4\mu \qquad \text{(D-2)}$$

where A, B, and C are given by Eqs. (30), (31), (32), and

$$F = -\lambda_E C_{D_{C_L^4}} \frac{8W^3}{\rho^3 S^3 V}\left[\frac{r_o^2}{Vr^2} - \frac{V}{g_o r}\right]^4 \qquad \text{(D-3)}$$

The Euler equations for $\dot{\lambda}_\chi$, $\dot{\lambda}_\varphi$, $\dot{\lambda}_\Lambda$, as given by Eqs. (25) to (27) do not change; however

$$\dot{\lambda}_E = \left\{3\lambda_E C_{D_o} \frac{\rho S V^2}{2W} + \lambda_\chi \frac{\sin\chi \tan\varphi}{r} + \lambda_\varphi \frac{\cos\chi}{r} - \lambda_\Lambda \frac{\sin\chi}{r\cos\varphi}\right\} \frac{\partial V}{\partial E}$$

$$+ \lambda_E C_{D_{C_L^2}} \frac{2W}{\rho S}\left[\frac{3V^2}{g_o^2 r^2} - \frac{r_o^4}{r^4 V^2} - \frac{2r_o^2}{g_o r^3}\right]\frac{\partial V}{\partial E}\sec^2\mu + \lambda_\chi\left[\frac{g_o r_o^2}{V^2 r^2} + \frac{1}{r}\right]\frac{\partial V}{\partial E}\tan\mu \quad \text{(D-4)}$$

$$+ \lambda_E C_{D_{C_L^4}} \frac{8W^3}{\rho^3 S^3 V^2}\left[\frac{5r_o^2}{Vr^2} + \frac{3V}{g_o r}\right]\left[\frac{r_o^2}{Vr^2} - \frac{V}{g_o r}\right]^3 \frac{\partial V}{\partial E}\sec^4\mu$$

where, as before,

$$\frac{\partial V}{\partial E} = \frac{g_o}{V} \quad \text{and} \quad V = \sqrt{2g_o\left(E + \frac{r_o^2}{r}\right)}$$

Bank angle is determined from $\partial H/\partial\mu = 0$ and results in the following cubic equation:

$$\tan^3\mu + \left[\frac{B + 2F}{2F}\right]\tan\mu + \frac{C}{4F} = 0 \quad \text{(D-5)}$$

where

$$\frac{B + 2F}{2F} = a = \frac{C_{D_{C_L^2}} \rho^2 V^2 S^2}{8C_{D_{C_L^4}} W^2\left[\frac{r_o^2}{Vr^2} - \frac{V}{g_o r}\right]^2} + 1 \quad \text{(D-6)}$$

$$\frac{C}{4F} = b = -\frac{\lambda_\chi g_o \rho^3 S^3 V}{32\lambda_E C_{D_{C_L^4}} W^3\left[\frac{r_o^2}{Vr^2} - \frac{V}{g_o r}\right]^3} \quad \text{(D-7)}$$

Thus $\tan^3\mu + a\tan\mu + b = 0$. The roots of this cubic equation depend on the sign of $(b^2/4 + a^3/27)$. It can be shown that this quantity is always positive, providing both C_D and C_D have
$\qquad\qquad\qquad\qquad\qquad\qquad\qquad\qquad\qquad\qquad\qquad\qquad\qquad\qquad\qquad\qquad C_L^2 \qquad\qquad C_L^4$
the same sign, and therefore there is only one real root (the other two are imaginary and can be ignored). Since both of these coefficients are positive, there is only one solution, namely

$$\tan\mu = G = \sqrt[3]{-\frac{b}{2} + \sqrt{\frac{b^2}{4} + \frac{a^3}{27}}} + \sqrt[3]{-\frac{b}{2} - \sqrt{\frac{b^2}{4} + \frac{a^3}{27}}} \qquad \text{(D-8)}$$

where a and b are given by Eqs. (D-6) and (D-7). Substitution of Eq. (D-8) into (D-2) results in

$$H = A + B + CG + F + BG^2 + 2FG^2 + FG^4 \qquad \text{(D-9)}$$

which, like Eq. (34), is a function of only one control variable, namely, r.

APPENDIX E

CONSTANTS OF THE MOTION FROM NOETHER'S THEOREM

Noether's theorem (Ref. 31) applies to variational problems that possess symmetry. Symmetry exists if one can subject a system of equations of motion to a certain operation (transformation) and the system appears exactly the same after the operation. For example, Noether's theorem shows that if the coordinate system that defines the state variables can be translated, rotated, or shifted in time without changing the dynamics of the problem then for each transformation a constant of the motion can be derived. This applies not only to the variational formulations of classical and quantum mechanics, for which the theorem was originally derived (Ref. 31), but also to modern optimal control problems (Ref. 32), for which the constants of the motion involve both state and multiplier variables.

The coordinate system for Eqs. (1) to (6) and the reduced system (11) to (14) are such that rotations about the three axes of the reference system which define Λ, φ, and χ can be made without affecting either the dynamics or the optimal solutions. This would not be true for the case with earth rotation, since a change in orientation of the earth's axis of rotation would result in different optimal trajectory solutions.

Using Noether's theorem, H. G. Moyer of the Grumman Research Department derived the following three constants:

$$C_1 = \lambda_\chi \cos \Lambda \sec \varphi - \lambda_\Lambda \cos \Lambda \tan \varphi + \lambda_\varphi \sin \Lambda \qquad \text{(E-1)}$$

$$C_2 = \lambda_\chi \sin \Lambda \sec \varphi - \lambda_\Lambda \sin \Lambda \tan \varphi - \lambda_\varphi \cos \Lambda \qquad \text{(E-2)}$$

$$C_3 = \lambda_\Lambda \qquad \text{(E-3)}$$

Writing these three equations in matrix form and inverting the square matrix, the multipliers are expressed in terms of latitude, longitude, and the three constants

$$\lambda_\chi = C_1 \cos \Lambda \cos \varphi + C_2 \sin \Lambda \cos \varphi + C_3 \sin \varphi \qquad \text{(E-4)}$$

$$\lambda_\Lambda = C_3 \qquad \text{(E-5)}$$

$$\lambda_\varphi = C_1 \sin \Lambda - C_2 \cos \Lambda \qquad \text{(E-6)}$$

where the determinant of the matrix given by (E-1) to (E-3) is sec φ, which is singular only when $\varphi = \pm 90°$ (crossrange exceeds 5000 nautical miles).

Equations (E-1) to (E-6) have been verified analytically for the complete system (1) to (6), the reduced system (11) to (14), and the reduced system (B-14) to (B-16) with energy as the independent variable.

The significance of the three constants of the motion is twofold. First, it eliminates the step-by-step numerical integration of $\dot{\lambda}_\chi$ and $\dot{\lambda}_\varphi$. Since $\lambda_\Lambda = C_3$, Eqs. (B-17), (B-19), (B-20) and (B-23) can be expressed in terms of the constants and state variables, thereby completely eliminating the use of multipliers for the energy-independent-variable system. Similarly, if advantage is taken of the fact that the Hamiltonian is constantly zero, the use of the multipliers for the time-independent-variable system is also eliminated. The difficulty in determining iteratively the numerical values of C_1, C_2, C_3 is no greater than determining the initial conditions of the multipliers, since

$$C_1 = \lambda_{\chi_o} \quad C_2 = -\lambda_{\varphi_o} \quad C_3 = \lambda_{\Lambda_o}$$

Care must be taken, however, that the right side of (E-4) goes to zero at the end of each optimal solution. Secondly, since the three constants are valid for the sixth-, fourth-, and third-order systems, as well as problems with any constraints imposed, it is possible to predetermine the values of the constants as a function of target conditions and store them in the vehicle's computer to be used as a basis for an on-board guidance scheme. The difficulty here is that the constants apply to a nonrotating earth and may have to be modified for the real world situation.

REFERENCES

1. Kaiser, F., "Der Steigflug mit Strahlflugzeugen-Teil 1, Bahngeschwindigkeit besten Steigens," Vefsuchsbericht 262-02-L44, Messerschmitt A. G., Augsburg, April 1944 (translated as Ministry of Supply RTP/TIB Translation GDC/15/148T).

2. Lippisch, A., "Flugmechanische Beziehungen der Flugzeuge mit Strahlantrieb," Air Material Command Translation Report No. F-TS-685-RE, October 1946.

3. Lush, K. J., "A Review of the Problem of Choosing a Climb Technique with Proposals for a New Climb Technique for High Performance Aircraft," Aeronautical Research Council Report Memo No. 2557, 1951.

4. Rutowski, E. S., "Energy Approach to the General Aircraft Performance Problem," Journal of the Aerospace Sciences, Vol. 21, No. 3, pp. 187-195, March 1954.

5. Miele, A., "Optimum Climbing Technique for a Rocket-Powered Aircraft," Jet Propulsion, Vol. 25, No. 8, August 1955.

6. Kelley, H. J., "Gradient Theory of Optimal Flight Paths," American Rocket Society Journal, Vol. 30, No. 10, October 1960.

7. Kelley, H. J., Kopp, R. E., and Moyer, H. G., "Successive Approximation Techniques for Trajectory Optimization," presented at the IAS Vehicle Systems Optimization Symposium, Garden City, New York, November 28-29, 1961.

8. Bryson, A. E. and Denham, W. F., "A Steepest-Ascent Method for Solving Optimum Programming Problems," Journal of Applied Mechanics, Vol. 29, No. 2, June 1962, pp. 247-257.

9. Kelley, H. J., Kopp, R. E., and Moyer, H. G., "A Trajectory Optimization Technique Based upon the Theory of the Second Variation," presented at the AIAA Astrodynamics Conference, Yale University, New Haven, Connecticut, August 19-21, 1963.

10. McGill, R. and Kenneth, P., "Solution of Variational Problems by Means of a Generalized Newton-Raphson Operator," AIAA Journal, Vol. 2, No. 10, October 1964, pp. 1761-1766.

11. Boyd, J. R., Christie, T. P., and Gibson, J. E., "Energy-Maneuverability (U)," Eglin Air Force Base, Florida, APGC-TR-66-4, March 1966 (SECRET).

12. Bryson, A. E., Desai, M. N. and Hoffman, W. C., "Energy-State Approximation in Performance Optimization of Supersonic Aircraft," Journal of Aircraft, Vol. 6, No. 6, November-December 1969, pp. 481-488.

13. Kelley, H. J. and Edelbaum, T. N., "Energy Climbs, Energy Turns and Asymptotic Expansions," Journal of Spacecraft and Rockets, Vol. 7, No. 1, January-February 1970, pp. 93-95.

14. Hedrick, J. K., "Optimal Three Dimensional Turning Maneuvers for Supersonic Aircraft," Ph.D. Dissertation, Department of Aeronautical and Astronautical Engineering, Stanford University, January 1971.

15. Connor, M. A., "Optimization of a Lateral Turn at Constant Height." AIAA Journal, Vol. 5, No. 2, February 1967, pp. 335-338.

16. Bryson, A. E. and Lele, M. L., "Minimum Fuel Lateral Turns at Constant Altitude," AIAA Journal, Vol. 7, No. 3, March 1969, pp. 559-560.

17. Hedrick, J. K. and Bryson, A. E., "Minimum Time Turns for a Supersonic Airplane at Constant Altitude," Journal of Aircraft, Vol. 8, No. 3, March 1971, pp. 182-187.

18. Hoffman, W. C. and Bryson, A. E., "A Study of Techniques for Real-Time, On-Line Optimum Flight Path Control — Minimum-Time Turns to a Specified Track," ASI-TR-71-4, Aerospace Systems, Inc., Burlington, Massachusetts, September 1971.

19. Bryson, A. E. and Hedrick, J. K., "Three Dimensional, Minimum-Time Turns for a Supersonic Aircraft," AIAA Paper No. 71-796, AIAA 3rd Aircraft Design and Operations Meeting, Seattle, Washington, July 1971.

20. Hedrick, J. K. and Bryson, A. E., "Three-Dimensional, Minimum-Fuel Turns for a Supersonic Aircraft," AIAA Paper No. 71-913, AIAA Guidance, Control and Flight Mechanics Conference, Hofstra University, Hempstead, New York, August 1971.

21. Kelley, H. J. and Lefton, L., "Supersonic Aircraft Energy Turns," 5th IFAC Congress, Paris, France, June 12-17, 1972.

22. Kelley, H. J., "Aircraft Maneuver Optimization by Reduced-Order Approximations," Advances in Control Systems - Vol. IX, edited by C. T. Leondes, Academic Press, 1972.

23. Kelley, H. J., "Singular Perturbations for a Mayer Variational Problem," AIAA Journal, Vol. 8, No. 6, June 1970, pp. 1177-1178.

24. Kelley, H. J., "Flight Path Optimization with Multiple Time Scales," Journal of Aircraft, Vol. 8, No. 4, April 1971, pp. 238-240.

25. "Alternate Space Shuttle Concepts Study — Part II Technical Summary — Volume II Orbiter Definition," Grumman/Boeing Final Report, MSC-03810, July 6, 1971.

26. Bryson, A. E. and Ho, Y. C., "Applied Optimal Control," Blaisdell Publishing Company, Waltham, Massachusetts, 1969.

27. Valentine, F. A., "The Problem of Lagrange with Differential Inequalities as Added Side Conditions," Dissertation, Department of Mathematics, University of Chicago, Chicago, Illinois, 1937.

28. Leitmann, G., "Variational Problems with Bounded Control Variables," Chapter 5 in Optimization Techniques, edited by G. Leitmann, Academic Press, 1962.

29. Miele, A., "Flight Mechanics - Vol. 1 - Theory of Flight Paths," Addison-Wesley Publishing Company, Reading, Massachusetts, 1962.

30. "Application of Numerical Methods to Extend Capabilities for Optimal Rocket Guidance," Final Report on Contract NAS 8-21315, IBM Federal Systems Division, Gaithersburg, Maryland, March 8, 1972.

31. Noether, E., "Invariante Variations Probleme," Nachrichten der Gesellschaft für Wissenschaft Göttingen, Vol. 1918, 1918, pp. 235-257.

32. Moyer, H. G., "Integrals for Impulsive Orbit Transfer from Noether's Theorem," AIAA Journal, Vol. 7, No. 7, July 1959, pp. 1232-1235.